Bioelectromagnetics 19:293–299 (1998)

Calculation of Electric Fields and Currents Induced in a Millimeter-Resolution Human Model at 60 Hz Using the FDTD Method

C. M. Furse[1]* and O. P. Gandhi[2]

[1]Department of Electrical and Computer Engineering, Utah State University, Logan Utah
[2]Department of Electrical Engineering, University of Utah, Salt Lake City, Utah

The finite-difference time-domain (FDTD) method has previously been used to calculate induced currents in anatomically based models of the human body at frequencies ranging from 20 to 915 MHz and resolutions down to about 1.25 cm. Calculations at lower frequencies and higher resolutions have been precluded by the huge number of time steps that would be needed in these simulations. This paper describes a method used to overcome this problem and efficiently calculate induced currents in an MRI-based, 6-mm-resolution model of the human under a high-voltage transmission line. This model is significantly higher resolution than the 1.31-cm-resolution model previously used; therefore, it can be used to pinpoint locations of peak current densities in the body. Proposed safety guidelines would allow external electric fields of 10 kV/m and 25 kV/m for exposure to 60 Hz fields of the general public and workers, respectively. For this external electric field exposure of 10 kV/m, local induced current densities as high as 20 mA/m^2 are found in the head and trunk with even higher values (above 150 mA/m^2) in the legs. These currents are considerably higher than the 4 or even 10 mA/m^2 that have been suggested in the various safety guidelines, thus indicating an inconsistency in the proposed guidelines. In addition, several ratios of E/H typical of power line exposures were examined, and it was found that the vertical electric field couples strongly to the body, whereas the horizontal magnetic field does not. Bioelectromagnetics 19:293–299, 1998.

Key words: numerical simulation; dosimetry; power lines; safety guidelines; electric field; induced currents; FDTD method

INTRODUCTION

This paper presents a more efficient method of computing induced currents at low frequencies using the finite-difference time-domain (FDTD) method. This method has been used extensively to calculate specific absorption rate (SAR) and induced currents in anatomically based models of the human body in the megahertz range [Chen and Gandhi, 1989; Gandhi et al., 1990; Gandhi et al., 1992]. It has also been used to examine current distribution in a 1.31-cm-resolution model at 60 Hz [Gandhi and Chen, 1992b].

Rather than using the pulsed FDTD method described in Gandhi and Chen [1992], the continuous wave FDTD method is used, with a novel time-to-frequency domain conversion. By using this technique, the induced electromagnetic fields (EMFs) and current distributions have been calculated for a grounded 6-mm-resolution MRI-based model of the human body for incident fields that may be encountered under ultra-high-voltage power transmission lines. A vertically polarized frontally incident plane wave is used to represent the power line. The wave has E = 10 kV/m and B = 33.3 μT from side to side of the model (E/H = 377 ohms), which is very typical of power line configurations [ORAU, 1992] and is the maximal recommended external electric field in proposed safety guidelines [CENELEC, 1995]. The separate effect of E and H was also examined, as described in section "Separation of Electric and Magnetic Fields," and it was found that the vertical E field contributes more dominantly than the magnetic field to the induced currents.

Contract grant sponsor: National Science Foundation; Contract grant number: BCS-9215274.

*Correspondence to: Cynthia M. Furse, Department of Electrical and Computer Engineering, Utah State University, Logan, Utah 84322-4120. E-mail: furse@alpha.ece.usu.edu

Received for review 30 August 1996; final revision received 8 December 1997

In this paper, we give the induced vertical currents calculated for the various layers of the model. The calculated currents are in excellent agreement with the experimental data of Deno [1977] and the previously calculated values for a 1.31-cm-resolution model [Gandhi and Chen, 1992]. This new 6-mm model is then used to obtain high-resolution definition of the current density distributions. Peak current densities and electric field magnitudes are calculated in each of the layers. For several regions of the body, the currents are found to be in excess of 4 or even 10 mA/m^2, which have been suggested as the upper limits of exposure in the safety guidelines proposed by an international working group of European Communities [Allen et al., 1991], CENELEC [1995], and by IRPA [1990].

APPLICATION OF THE FDTD METHOD TO LOW-FREQUENCY SIMULATIONS

Several challenges are unique to low frequency FDTD simulations. First is how to obtain accurate information for the fields inside the body, which are several orders of magnitude lower than the external fields and are therefore very susceptible to numerical round-off errors. Second is how to obtain the magnitude and phase of the resultant low-frequency fields, as it is impractical, impossible, or inaccurate to run the simulation for a full cycle of the waveform. The third issue is the use of absorbing boundary conditions. These issues are discussed in turn to explain the use of the FDTD method for low-frequency high-resolution simulations.

Use of Frequency-Scaling to Improve the Accuracy of Quasi-Static FDTD Simulations

For low-frequency bioelectromagnetic simulations, such as those at 60 Hz, even the most dominant fields in the body are several orders of magnitude lower than the external fields. This is because of the continuity of the electric flux density ($\mathbf{D} = \varepsilon\mathbf{E}$) from exterior to interior of the body and because the complex dielectric constant of human tissues is several million times larger than that of the air outside. This combination results in significant round-off errors in the internal fields. Use of double precision reduces this problem but does not eliminate it, and requires twice the memory requirement of single-precision calculations. An effective way to reduce this problem is to use the method of frequency scaling [Kaune and Gillis, 1981; Guy et al., 1982; Gandhi and Chen, 1992], which relies on the quasi-static nature of the problem. This method is applicable when the size of the body is a factor of 10 or more smaller than the wavelength and $|\sigma + j\omega\varepsilon| \gg \omega\varepsilon_o$, where σ and ε are the conductivity and the permittivity of the tissues, respectively, $\omega = 2\pi f$ is the radian frequency, and ε_o is the permittivity of the free space outside the body. Under these conditions, the electric fields in air are normal to the body surface, and the internal tissue electric fields are given from the boundary conditions in terms of the fields outside:

$$j\omega\varepsilon_o\mathbf{n}\cdot\mathbf{E}_{air} = (\sigma + j\omega\varepsilon)\mathbf{n}\cdot\mathbf{E}_{tissue}.$$

A higher quasi-static frequency f′ may therefore be used for irradiation of the model, and the internal fields $\mathbf{E}'$ thus calculated may be scaled back to frequency f of interest, e.g., 60 Hz:

$$E = \frac{f}{f'}E' \tag{1}$$

This method has been shown to be very accurate for homogeneous or layered spheres (diameter = 33 cm) up to about 20 MHz [Gandhi and Chen, 1992]. The fields ($\mathbf{E}'$), which are calculated at the higher frequency (f′) using frequency scaling, are several orders of magnitude higher than $\mathbf{E}$, which would have been calculated at the low frequency (f), and therefore have less numerical round off error. In this paper, the simulations are run at f′ = 10 MHz and are scaled to f = 60 Hz, which is consistent with the method demonstrated in Gandhi and Chen [1992].

Boundary Conditions

The absorbing boundary conditions are a potential source of error for low-frequency simulations, as the distance between these boundaries and the body is very small compared with a wavelength. It has been shown that the perfectly matched layer (PML) boundary condition can be used accurately at low frequencies and that Mur boundary conditions are stable, but give reflections up to 20% larger than the PML boundary conditions [De Moerloose and Stuchly, 1996]. To assess how much error these reflections induce in a realistic simulation, a comparison was made between an eight-layer PML boundary of order 2.1, optimized as in Lazzi and Gandhi [1997], and the retarded time boundary condition [Berntsen and Hornsleth, 1994] nine cells away from the scatterer. Results are discussed in the "Validation of the Methods" section below. The PML condition was found to give slightly more accurate results, although it was observed that both boundary conditions performed well enough to provide less than 7% error for the electric field components anywhere within the sphere.

Calculation of Magnitude and Phase

For high-resolution, low-frequency simulations, a cycle of the wave is made up of a huge number of time steps. Using a resolution of 6 mm, for instance, a 60 Hz wave has 1.67×10^9 time steps, and a 10

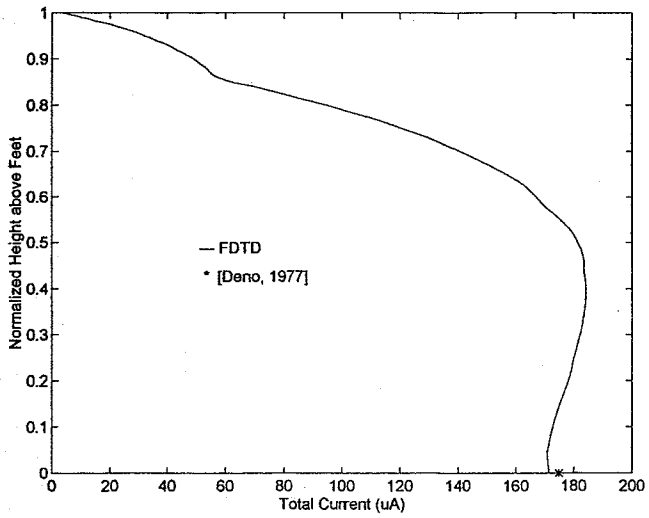

Fig. 1. The calculated vertical currents passing through the various sections of a 6 × 6 × 6 mm MRI-based grounded model of the human body exposed to EMFs at 60 Hz. E_{inc} = 10 kV/m, vertically polarized, frontally incident; B_{inc} = 33.3 μT from side to side of the model. Note the excellent agreement with the experimental data of Deno [1977].

MHz wave has 10,000 time steps. The method used in Gandhi and Chen [1992] was to run a complete cycle of this wave and obtain the magnitudes of the wave from peak detection. It should first be noted that the simulation converges in far less than one cycle, because convergence is based on elapsed time and number of reflections, not on the wave itself. Rather than running an entire cycle of the simulation, a more efficient method is to calculate the magnitude from two time steps beyond convergence. This direct method is based on writing two equations in two unknowns (magnitude and phase) for the time-domain fields, and then solving them directly for the magnitude and phase. At a given location in space, two equations can be written for two unknowns, A and θ:

$$A \sin(\omega t_1 + \theta) = q_1$$
$$A \sin(\omega t_2 + \theta) = q_2 \qquad (2)$$

where A is the magnitude, θ is the phase angle, and ω (=2πf) is the angular frequency. At two times, t_1 and t_2, the field component values q_1 and q_2 are obtained from the FDTD simulation, and these two equations can be solved directly for the two unknowns, magnitude and phase.

The choice of t_1 and t_2 depends on the simulation. Although round-off errors will be minimized when t_1 and t_2 are a quarter cycle apart, sufficient accuracy can usually be obtained when they are far closer, thus improving the efficiency of the simulations. For the simulations in this paper, t_1 and t_2 are taken to be 100 time steps apart (0.01 cycle in 6-mm-resolution simulations at 10 MHz).

This method is highly efficient and accurate for all frequencies, provided that the output of the simulation is a clean, converged sine wave (or any part thereof). Fortunately, noise and DC offsets, which have been shown to cause errors in some FDTD simulations [Furse, 1994; Buechler et al., 1995], do not appear in the simulations performed for this paper. This absence is because the resolution is so high compared with wavelength that the turn-on of the wave is very slow (in fact, nearly a linear ramp), which has been shown to eliminate these problems [Buechler et al., 1995; Furse, 1994].

SEPARATION OF ELECTRIC AND MAGNETIC FIELDS

Underneath high-voltage power lines, the ratio of electric and magnetic fields ranges from 420 to 1500 ohms [ORAU, 1992]. To analyze the effect of these varying electric and magnetic fields, we used a method similar to De Moerloose and Stuchly [1996] in which two plane wave simulations were made, one from the front and one from the back. These simulations were

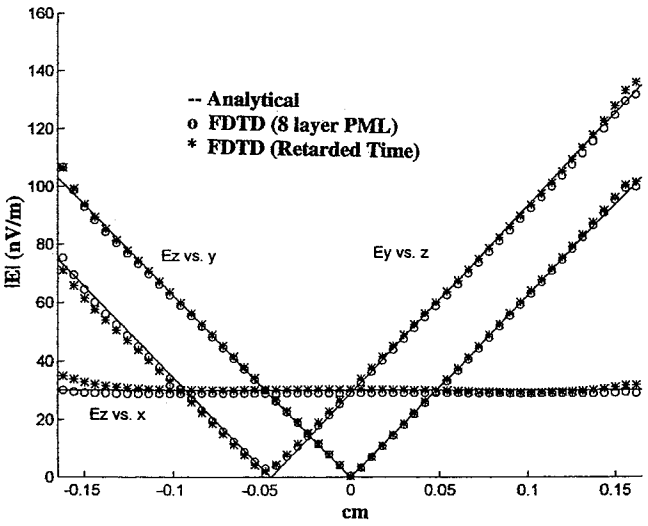

Fig. 2. Comparison of analytical and FDTD results for a brain-equivalent sphere, ε_r = 1.0, σ = 0.35 S/m, radius = 16.5 cm. The FDTD simulation was run at 20 MHz for 1000 time steps using the two-equations two-unknowns method to obtain magnitudes of the fields, and these values were scaled to 60 Hz using the method of frequency scaling. Two FDTD simulations are compared with the analytical solution. One simulation is made with the retarded time boundary condition nine cells away from the sphere, and the second simulation was made with an eight-layer PML boundary condition (of order 2.1) seven cells away from the sphere. $\mathbf{E}_{inc}$ = 1 V/m, $\mathbf{H}_{inc}$ = 1/377 A/m.

TABLE 1. Conductivities of the Tissues in the 6-mm-Resolution Human Model for 60 Hz*

Tissue	Conductivity σ (S/m)
Muscle (horizontal)	0.068
Muscle (vertical)	0.86
Fat	0.037
Compact bone; Bone marrow; Cartilage	0.019
Blood	0.60
Pancreas	0.143
Intestine; Pancreas; Spleen	0.11
Brain; Pituitary gland; Pineal gland; Parotid gland	0.17
Nerve/Spinal Cord	0.69
Liver	0.12
Kidney	0.27
Lung	0.078
Heart	0.5
Skin	0.11
Eye Humor	1.5
Eye sclera; Eye lens	0.11
CSF	1.5
Bladder	0.17
Stomach	0.11
Ligament	0.11
Testicle; Spermatic cord; Prostate gland	0.11
Erectile tissue	0.6

*Values taken from Geddes and Baker [1967] and Zheng et al. [1984]. The value of $\varepsilon_r = 1.0$ was used for these simulations.

superimposed (added), effectively isolating the electric and removing the magnetic fields.

As an alternative, we ran two plane waves from the same direction (frontally incident), one right-handed and one left-handed, by programming the FDTD algorithm with a slight change of signs. In the right-handed simulation, a plane wave travelling in the $-y$ direction (frontally incident) has $+E_z$ and $+H_x$. The left-handed simulation has $+E_z$ and $-H_x$. The complex fields at all locations are stored from both of these simulations, and the superimposition (addition) of these waves effectively isolates the electric and removes the magnetic fields (or when subtracted, removes the electric and isolates the magnetic fields). Using the principle of superposition, any ratio of E and H can be analyzed.

This method was tested on the simulation of currents and fields in a 6-mm-resolution model of the human body. The model was exposed to a vertically polarized $E_z = 10$ kV/m frontally incident plane wave. The simulation was run for 2000 time steps, and then scaled to 60 Hz using Eq. (1), and the current densities were found from

$$J_z = \sigma_z E_z(t). \tag{3}$$

Displacement current was neglected because of the extremely low frequency.

The total vertical current passing through each layer is shown in Figure 1.

Several simulations were then compared for E/H = 10, 50, 377, 700, and 1000. The current distribution shown in Figure 1 is the same to the fourth decimal place for all of these simulations. The currents were also calculated with strictly the E field, which gave the same results as Figure 1 to within the fourth decimal place. This set of tests indicates that the vertical electric field couples strongly to the body at low frequencies, whereas the horizontal magnetic field does not. The ratio of E and H is insignificant, and the magnitude of the electric field is of primary importance when calculating induced currents from fields with this polarization. Thus, a plane wave, which is simple to run, was used in the following simulations. It is worthwhile to note that the ratio of E and H seems to be more significant at higher frequencies, where the magnetic field also couples to the body.

VALIDATION OF THE METHODS

To show that the methods described above will give accurate calculations for the fields inside the human body, we have used a canonical problem that was previously considered by Gandhi and Chen [1992]. They used a torso-equivalent sphere model to demonstrate the accuracy of the frequency scaling method described above. We extend this test case to demonstrate the accuracy of the FDTD approach using frequency scaling and two different absorbing boundary conditions. A 16.5-cm radius torso-equivalent sphere with $\sigma = 0.35$ S/m and $\varepsilon_r = 1.0$ was simulated with FDTD using a 20 MHz sinusoidal plane wave. It was run for 1000 time steps (instead of 10,000 time steps in Gandhi and Chen [1992]) using the two-equations two-unknowns method for obtaining magnitudes. Two different boundary conditions were used, namely the retarded time conditions and the PML conditions, as previously defined. Boundaries were located nine and seven cells from the sphere, respectively. The resolution of the simulation is $\Delta = 6$ mm along each of the orthogonal axes. The fields obtained from this simulation were scaled to 60 Hz using (1). The results are shown in Figure 2, where they are compared with the quasi-static analytical solution obtained from electrostatics and magnetostatics for incident E and H, respectively. The agreement is excellent, lending support to the validity of using the scaled-frequency FDTD method to obtain induced fields at power-line and other ELF frequencies.

MILLIMETER-RESOLUTION MODEL OF THE HUMAN BODY

In collaboration with Dr. James Lee of the Medical Imaging Laboratory, University of Utah School of Medi-

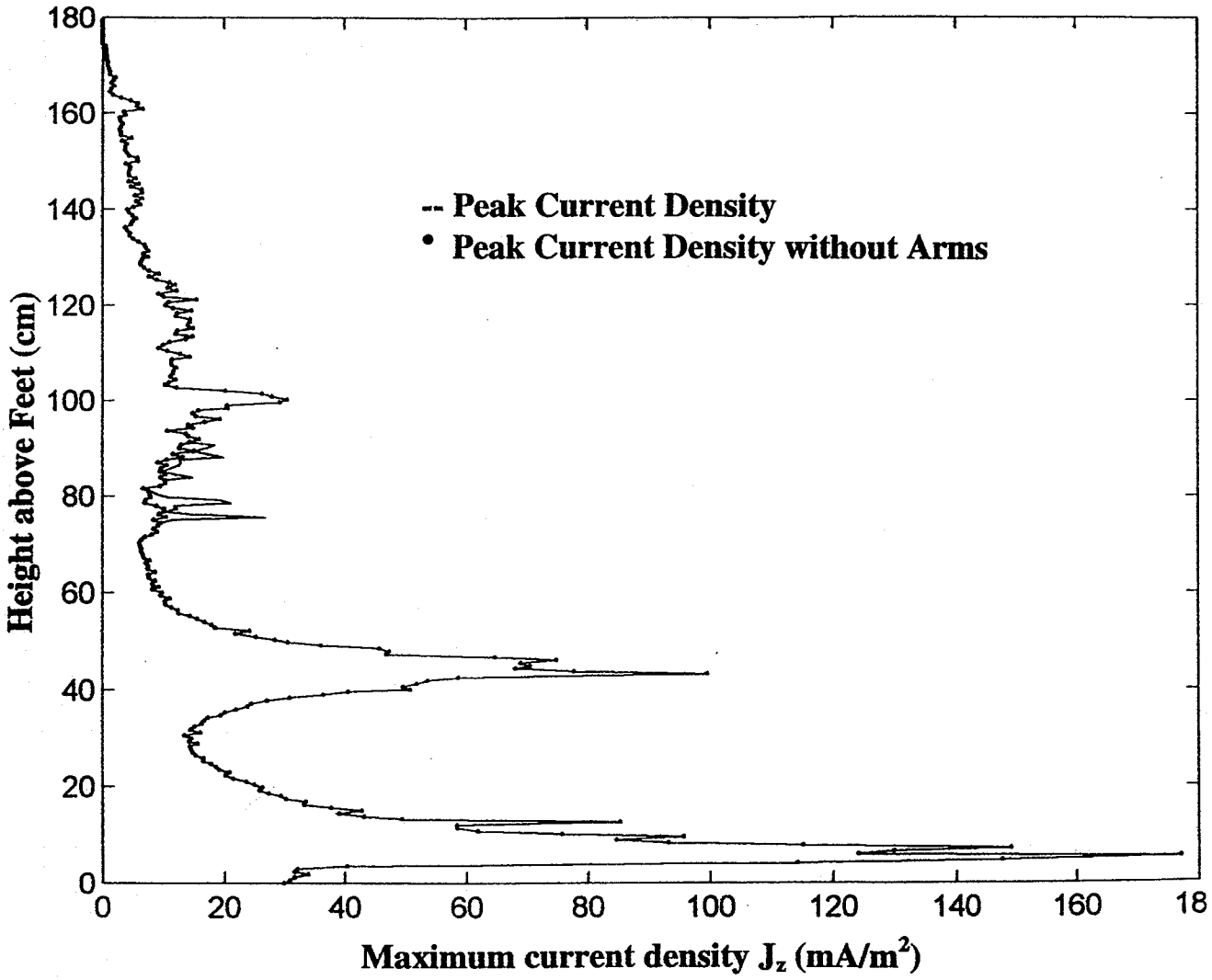

Fig. 3. The calculated maximal current densities induced in each of the sections of the 6-mm-resolution grounded model. E_{inc} = 10 kV/m, vertically polarized, frontally incident; B_{inc} = 33.3 μT from side to side of the model.

cine, and Professor Mark Nielson of the Department of Biology, University of Utah, we have developed a new millimeter-resolution model of the human body. It is based on magnetic resonance imaging (MRI) scans of a male volunteer of height 176.4 cm and weight 64 kg. The MRI scans were taken with a resolution of 3 mm along the height of the body (vertical axis) and 1.875 mm for the orthogonal axes in the cross-sectional planes. Even though the height of the volunteer was quite appropriate for an average adult male, the weight was somewhat lower than the average of 71 kg, which is generally assumed for an average male. This problem can, to some extent, be ameliorated by assuming that the cell dimensions for the cross-sections are larger than 1.875 mm by a ratio of $(71/64)^{1/2} = 1.053$. By taking the larger cell dimensions of $1.053 \times 1.875 = 1.974$ mm for the cross-sectional axes, the volume of the model can be increased by $(1.053)^2 = 1.109$, i.e., by about 10.9%. The change in volume results in an increase of its weight by approximately the same percentage, i.e., to a new weight of 71 kg.

The MRI sections were converted to images involving 30 tissue types, whose electrical properties can then be prescribed at the irradiation frequency. The tissue types and their conductivities at 50–60 Hz [Geddes and Baker 1967; Zheng et al., 1984] are listed in Table 1. The value of ε_r is relatively insignificant in low frequency biological simulations, because the conduction component of the complex dielectric constant $\sigma/(\omega\varepsilon_r\varepsilon_o)$ is much larger than the displacement component ε_r. Therefore, ε_r is taken to be 1.0 in these simulations. The pineal gland is suspected of being involved in the bioeffects of power-frequency EMFs and has

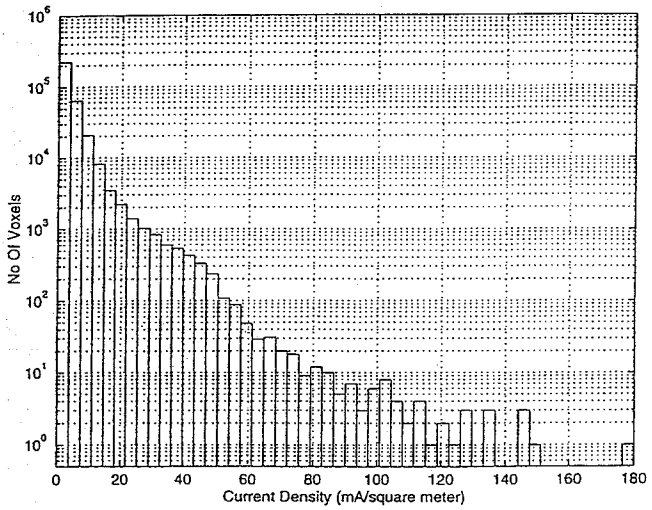

Fig. 4. Histogram of current densities induced in the body for the 6-mm-resolution grounded model. E_{inc} = 10 kV/m, vertically polarized, frontally incident; B_{inc} = 33.3 μT from side to side of the model.

therefore been separately identified for calculation of induced electric fields and current densities. Because it is impossible to run the 1.974 × 1.974 × 3-mm-resolution model of the whole body with the computer memories of readily available computing workstations (64–512 Mbytes), we have combined 3 × 3 × 2 cells (taking the dominant tissue in each group) of the millimeter-resolution model to obtain a new, coarser, MRI-based model of dimensions 5.922 × 5.922 × 6 mm along the x-, y-, and z-directions, respectively. With nine cells to the retarded time absorbing boundary condition and a perfectly conducting ground plane under the feet, the model requires a calculation space of 107 × 75 × 316 or approximately 2.54 million cells.

CALCULATION OF CURRENTS AND FIELDS IN THE HUMAN MODEL

To simulate the currents and fields in the 6-mm-resolution model of the human body under a high-voltage transmission line, the model was exposed to a vertically polarized E_z = 10 kV/m frontally incident plane wave. Values for a 25 kV/m wave can be found by multiplying the current density values in the figures and tables by 2.5. As described in the "Separation of Electric and Magnetic Fields" section, the plane wave is a good representation of fields under the power line because of the minimal coupling of the horizontal magnetic field component. This value of electric field was chosen to represent the limit for external field for public exposures in proposed safety guidelines [CENELEC, 1995]. The simulation was run for 2000 time steps, and the electric-field magnitudes were found from time steps n_1 = 1900 and n_2 = 2000. They were then scaled to 60 Hz using Eq. (1), and the current densities were found from Eq. (3). Displacement current was neglected because of the extremely low frequency.

Values obtained from this simulation agree well with measured data from Deno [1977] as shown in Figure 1. The magnitude of the peak current density $(J_x^2 + J_y^2 + J_z^2)^{1/2}$ in each layer was calculated; these are plotted in Figure 3. The location of these peaks was

TABLE 2. Comparison of Endogenous Current Densities Induced in Prominant Organs by the Beating Heart* and the Exogenous Current Densities Induced by High Voltage (E = 10 kV/m) Power Lines**

	Endogenous current densities			Exogenous current densities		
Tissue	Jmin	Jav	Jmax	Jmin	Jav	Jmax
Intestine	9	86	460	406	1346	4745
Spleen	84	207	485	608	1378	3292
Pancreas	113	344	634	876	1461	3136
Liver	44	380	4577	577	1366	4659
Kidney	38	175	447	900	2760	5630
Lung	24	543	19 354	188	630	2616
Bladder	11	35	73	776	1913	4069
Heart			162 635	642	2198	5383
Stomach	106	614	6580	497	1258	2957
Testicles	1	7	17	108	689	1873
Prostate	11	18	25	366	1056	1758
Eye humor	4	22	82	192	5574	13 560
Cerebrospinal fluid	2	26	118	1010	4808	7187
Pineal gland	6	6	6	1451	1451	1451
Pituitary gland	3	3	3	3507	3507	3507
Brain	0.3	8	164	718	1881	8329

*Hart and Gandhi, manuscript submitted for publication.

**Values for 25 kV/m lines can be found by multiplying these current densities by 2.5. Current densities are given in μA/m².

observed graphically, to ensure that these were not spurious fields on the surface. In fact, they were all located deep within the body. In the region containing the arms, the peak current density was located inside the arms. Peak current densities in the torso are indicated by the dotted line in Figure 3. The peak current densities in the torso region are in excess of the 4 mA/cm^2 or even 10 mA/cm^2, which have been recommended by the various safety guidelines [Allen et al., 1991; IRPA, 1990]. To give an idea how the magnitudes of the current densities vary throughout the body, Figure 4 shows a histogram of the peak current densities in the voxels in the body.

In addition, the maximal and average calculated current densities in each organ were compared with the endogenous current densities, which are naturally generated by the beating heart (Hart and Gandhi, manuscript submitted for publication). Because the heartbeat contains numerous frequencies, only those frequencies in the range 40–70 Hz were considered. Table 2 gives a comparison of these values. It is observed that the current densities induced for the 10 kV/m plane-wave source (which is typical of fields underneath a high-voltage line under the proposed safety guidelines [IRPA, 1990; CENELEC, 1995] are considerably higher than the endogenous values.

CONCLUSIONS

The finite-difference time-domain method was used to find the electric fields and current densities inside a 6-mm-resolution model of the human body exposed to the fields which would be typical under a high-voltage power line. Various ratios of E/H were examined, and it was found that the vertical electric field couples strongly to the body, whereas the horizontal magnetic field does not. For incident external electric fields of 10 kV/m, which are allowed under proposed safety guidelines, local induced current densities as high as 20 mA/m^2 are found in the head and trunk with even higher values (above 150 mA/m^2) in the legs. Current densities 2.5 times higher would be observed for 25 kV/m fields. The current densities induced by the high-voltage lines at either 10 kV/m or 25 kV/m were also compared with those induced naturally by the beating heart, and it was found that the induced current densities are considerably higher than the endogenous ones.

ACKNOWLEDGMENTS

This work was supported by the National Science Foundation Grant BCS - 9215274. Computer time was provided by the Utah Supercomputing Institute.

REFERENCES

Allen SG, Bernhardt JH, Driscoll CMH, Grandolfo M, Mariutti GF, Matthes R, McKinlay AF, Steinmetz M, Vecchia P, Whillock M (1991): Proposals for basic restrictions for protection against occupational exposure to electromagnetic non-ionizing radiations: Recommendations of an international working group set up under the auspices of the Commission of European Communities. Physica Medica VII:77–89.

Berntsen S, Hornsleth SN (1994): Retarded time absorbing boundary conditions. IEEE Trans on Antennas and Propagation 42:1059–1064.

Buechler DN, Roper DH, Christensen DA, Durney CH (1995): Modeling sources in the FDTD formulation and their use in quantifying source and boundary condition errors. IEEE Trans on Microwave Theory and Techniques 43(4).

CENELEC European Pre-standard (1995): Human Exposure to Electromagnetic Fields - Low Frequency (0 Hz to 10 kHz): 1—23. Available from CENELEC Central Secretariat: reu de Stassart 35, B-1050 Brussels, Belgium.

Chen JY, Gandhi OP (1989): RF currents induced in an anatomically based model of a human for plane-wave exposures 20-100 MHz. Health Phys 57:89–98.

De Moerloose J, Stuchly MA (1996): Reflection analysis of PML-ABCs for low frequency applications. IEEE Microwave and Guided Wave Letters 6:344–346.

Deno DW (1977): Currents induced in the human body by high-voltage transmission line electric field: Measurement and calculation of distribution and dose. IEEE Trans on Power Apparatus and Systems 96:1517–1527.

Furse CM (1994): Use of the Finite Difference Line Domain Method for Broad Band Calculations of Electromagnetic Scattering and Absorption from Large Heterogeneous Objects, PhD dissertation, University of Utah.

Gandhi OP, Chen JY (1992): Numerical dosimetry at power-line frequencies using anatomically based models. Bioelectromagnetics 1(Suppl.):43–60.

Gandhi OP, Gu YG, Chen JY (1990): SAR and induced current distributions in anatomically based models of a human for plane-wave exposures at frequencies 20–915 MHz. Final Report submitted to Department of Microwave Research, Walter Reed Army Inst. of Research, Washington, D.C. 20307-3100, Contract No. DAMD 17-90-M-SA49, August 27, 1990.

Gandhi OP, Gu YG, Chen JY, Bassen HI (1992): Specific absorption rates and induced current distributions in an anatomically based human model for plane-wave exposures. Health Phys 63:281–290.

Geddes LA, Baker LE (1967): The specific resistance of biological material: A compendium of data for the biomedical engineer and pathologist. Med Biol Eng 5:271–293.

Guy AW, Davidow S, Yang GY, Chou CK (1982): Determination of electric current distributions in animals and humans exposed to a uniform 60-Hz high intensity electric field. Bioelectromagnetics 3:47–71.

IRPA (1990): Interim guidelines on limits of exposure to 50/60 Hz electric and magnetic fields. Health Phys 58:113–122.

Kaune WT, Gillis MF (1981): General properties of the interaction between animals and ELF electric fields. Bioelectromagnetics 6:13–32.

Lazzi G, Gandhi OP (1997): On the optimal design of the PML absorbing boundary condition for the FDTD code. IEEE Trans Antennas and Propagation. 5:914–916.

ORAU (1992): Health Effects of Low Frequency Electric and Magnetic Fields. Oak Ridge Associated Universities Panel for the Committee on Interagency Radiation Research and Policy Coordination, June 1992.

Zheng E, Shao S, Webster JG, (1984): Impedance of skeletal muscle from 1 Hz to 1 MHz. IEEE Trans Biomed Eng 31:477–481.